

Macromolecular crystallography at Elettra: current and future perspectives

Raghurama P. Hegde,^a Nicola Demitri,^a Annie Héroux,^b Alessandro Olivo,^a Giorgio Bais,^a Michele Cianci,^c Paola Storici,^a Dan-George Dumitrescu,^d Nishant Kumar Varshney,^e Balasubramanian Gopal,^f D. D. Sarma,^g Lisa Vaccari,^a Silvia Onesti^a and Maurizio Polentarutti^{a*}

Received 4 December 2024

Accepted 5 February 2025

Edited by M. Szebenyi, Cornell University, USA

This article forms part of a virtual issue celebrating the 50th Anniversary of the Stanford SSRL synchrotron radiation and protein crystallography initiative led by Keith Hodgson.

Keywords: data collection; X-ray diffraction; macromolecular crystallography; Elettra upgrade.

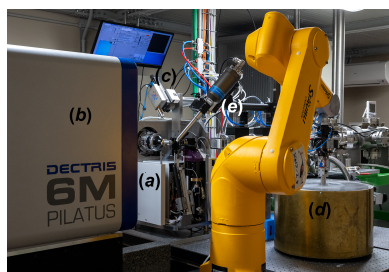
^aElettra – Sincrotrone Trieste SCpA, SS 14 km 163,5 in AREA Science Park, Basovizza, 34149 Trieste, Italy, ^bFormer Elettra – Sincrotrone Trieste SCpA, SS 14 km 163,5 in AREA Science Park, Basovizza, 34149 Trieste, Italy, ^cDepartment of Agricultural, Food and Environmental Sciences, Università Politecnica delle Marche, via Brecce Bianche 10, 60131 Ancona, Italy, ^dNobian, Van Asch v. Wijkstraat 53, 3811 LP Amersfoort, The Netherlands, ^eIR Technology Services Pvt Ltd, EL-91, TTC Industrial Area, Electronic Zone, Mahape, Navi Mumbai, Maharashtra 400710, India, ^fMolecular Biophysics Unit, Division of Biological Sciences, Indian Institute of Science, Bengaluru 560012, India, and ^gSolid State and Structural Chemistry Unit, Indian Institute of Science, Bengaluru 560012, India. *Correspondence e-mail: maurizio.polentarutti@elettra.eu

The Elettra synchrotron radiation facility, located in Trieste, Italy, is a third-generation storage ring, operating in top-up mode at both 2.0 and 2.4 GeV. The facility currently hosts one beamline fully dedicated to macromolecular crystallography, XRD2. XRD2 is based on a superconducting wiggler, and it has been open to users since 2018. On-site and remote access for data collection, as well as monitoring tools and automatic data analysis pipelines are available to its users. In addition, since 1994 Elettra has operated a general-purpose diffraction beamline, XRD1, offering the macromolecular community a wide spectrum extending to long wavelengths for phasing and ion identification. Ancillary facilities support the beamlines, providing sample preparation and a high-throughput crystallization platform for the user community. A new CryoEM facility is being established on campus and jointly operated by the Consiglio Nazionale della Ricerche – Istituto Officina dei Materiali (CNR–IOM) and Elettra, providing further opportunities to the Elettra user community. This review outlines the current capabilities and anticipated developments for macromolecular crystallography at Elettra to accompany the upcoming upgrade to Elettra 2.0, featuring a six-bend enhanced achromat lattice. The new source is expected to deliver a high-brilliance beam, enabling the macromolecular crystallography community to better address the emerging and future scientific challenges.

1. Introduction

Elettra-Sincrotrone Trieste (henceforth referred to as Elettra) is an Italian non-profit organization of national interest that oversees a multidisciplinary research centre of excellence. Its third-generation synchrotron source, Elettra, has been operational since 1993. Elettra currently powers 28 experimental stations, providing access to cutting-edge instruments for advanced spectroscopy, scattering and imaging techniques. Elettra has consistently enhanced its performance through regular upgrades to its ring, its beamlines, and its experimental stations.

Elettra is currently the only synchrotron radiation facility that regularly operates at two distinct energy levels, 2.4 and 2.0 GeV, depending on users' requirements for hard X-rays or VUV photons. Additionally, it offers a hybrid mode for time-resolved experiments. Out of its 28 beamlines, 9 are dedicated



to hard X-rays, 18 operate within the UV, soft, and tender X-ray range, and 1 focuses on the IR-THz range.

A number of beamlines have been built and are being operated in collaboration with national and international institutions and research centres. Nine beamlines are managed by the Italian National Research Council (CNR), including the X-ray diffraction beamline XRD1. Several international institutions have established beamlines at Elettra. The SAXS beamline was built by the Austrian Academy of Sciences and currently run together with the Institute of Inorganic Chemistry (Graz University of Technology). The Materials Science beamline was built and is run by Charles University in Prague, and the macromolecular crystallography XRD2 and the high pressure diffraction XPRESS beamlines were built and now run in partnership with the Indian scientific community via the Department of Science and Technology and Indian Institute of Science in Bangalore. The NanoESCA, SuperESCA and XRF beamlines are operated in partnership with institutions from Germany, Romania and the International Atomic Energy Agency (IAEA), respectively.

Approximately 80% of the beam time at Elettra (~6400 h per year) is allocated to the user community, based on the ranking of user proposals by international peer-review panels (Franciosi & Kiskinova, 2023). In 2024, over 500 scientists visited Elettra to conduct research spanning a variety of scientific fields. More than half of the users come from non-Italian institutions, with growing participation from Central-Eastern European and developing countries, thanks to ongoing collaborations with the Central European Initiative (CEI), the International Atomic Energy Agency (IAEA), the International Centre for Theoretical Physics (ICTP), the Central European Research Infrastructure Consortium CERIC-ERIC and the Lightsources for Africa, The Americas, Asia, Middle East and Pacific (LAAAMP) exchange programme. In the last five years, research conducted at the facility has resulted in more than 3000 scientific publications.

Elettra is undergoing a major upgrade to Elettra 2.0 (Karantzoulis *et al.*, 2024; Gregoratti *et al.*, 2024), a next-generation diffraction-limited light source expected to be operational from January 2027, offering enhanced brilliance and coherence. In this context, the present XRD2 beamline, dedicated to macromolecular crystallography, will be replaced by a new beamline (μ XRD). The upgrade integrates with a broader expansion of the Elettra's structural biology platforms funded by the NextGenerationEU programme, through the PRP@CERIC project (<https://www.pathogen-ri.eu>). This includes enhanced crystallization and protein characterization facilities, as well as the establishment of a new CryoEM facility, in collaboration with the CNR Istituto Officina dei Materiali.

2. Macromolecular crystallography (MX) at Elettra: current status

Prior to 2018 MX data collection was carried out at XRD1, a general-purpose diffraction beamline, that acted as an incubator, fostering multiple scientific communities and opening

the way to dedicated lines such as XRD2 for MX and Xpress for high pressure diffraction (Lausi *et al.*, 2015). The MX dedicated XRD2 beamline has been designed and realized as a partnership between Elettra and the Department of Science and Technology (DST), India/Indian Institute of Science (IISc, Bangalore). From its inception, XRD2 was designed with modern features essential for an MX beamline, focusing on stability and automation capabilities for remote access and operation. Several models were taken into consideration before adopting the final beamline layout and software environment. XRD2 went officially into operation in September 2018.

2.1. The macromolecular crystallography XRD2 beamline

The source for XRD2 is a superconducting wiggler delivering beam in parallel to three beamlines of which XRD2 is the central branch. The photon-delivery system provides at the sample position a native beam of $290 \mu\text{m} \times 90 \mu\text{m}$ ($h \times v$, FWHM) with a flux of 1.7×10^{12} photons s^{-1} (12.4 keV). The beam energy can be tuned between 8 and 20 keV, suitable for single- and multi-wavelength anomalous dispersion (SAD/MAD) phasing. The experimental station (Fig. 1) is equipped with an automounter system, coupled with a dewar hosting up to 192 samples, an Arinax MD2-S diffractometer, and a Dectris Pilatus 6M detector. Since 2020, most users are performing their experiments remotely, using the web application *MXCuBE3* for beamline control (Mueller *et al.*, 2017), *Braggy* for diffraction images inspection (<https://gitlab.esrf.fr/ui/h5web-braggy>) and *SynchWeb/ISPyB* (Fisher *et al.*, 2015; Delagenière *et al.*, 2011) as electronic logbook (Fig. 2).

2.1.1. Beamline source

XRD2 exploits as a source a 3.5 T cryo-cooled (He) superconducting wiggler (SCW, Table 1) with a large emitting cone limited to 2.0 mrad and 0.2 mrad (horizontal and

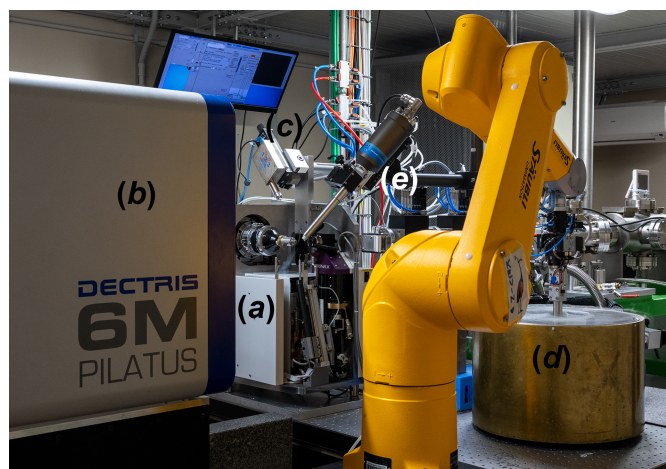


Figure 1
XRD2 experimental station consisting of (a) the Arinax MD2-S micro-diffractometer, (b) Pilatus 6M detector, (c) fluorescence detector, (d) automounter and (e) cryostream.

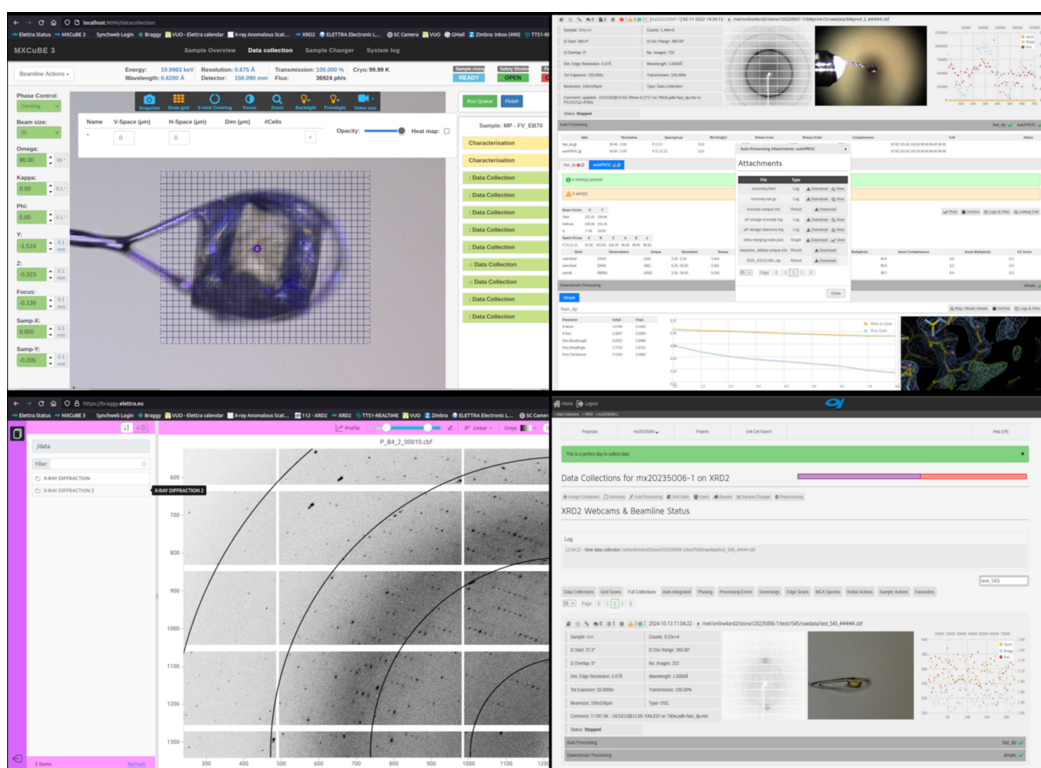


Figure 2

A composite image of the web-based software tools available to remote and in-person users at the XRD2 beamline showing (counterclockwise starting from top-left): *MXCuBE3* beamline control interface, visualization software for diffraction images, *Braggy*, and *SynchWeb/ISPyB* data logbook showing some results from autoprocessing of data (*fastdp/autoPROC/Dimple*).

vertical directions, respectively). The source offers wide, intense spectra extending well beyond 50 keV. The divergence of the radiation cone enables the beam to be split, serving as a source for two additional branch beamlines, each accom-

modating a radiation cone of $0.5 \text{ mrad} \times 0.2 \text{ mrad}$. The central portion of the beam, spanning $1.0 \text{ mrad} \times 0.2 \text{ mrad}$, is utilized by XRD2. Cryo-cooled silicon (111) crystals intercept the incoming beam and propagate fixed-energy photon beams at 25 keV and 13 keV for the Xpress and the incoming HF-SAXS beamlines, respectively.

Table 1

Source and optical layout details for XRD2 macromolecular crystallography beamline.

Source	
Period length	64 mm
Peak field	3.5 T
Total number of poles	49
Pole sequence	$1/4, -3/4, 1, -1, \dots, 1, -3/4, 1/4$
Internal aperture	$81 \text{ mm (H)} \times 10.7 \text{ mm (V)}$
Total power	18.3 kW (2 GeV, 400 mA)
Optics	
Collimating mirror	Cylindrical mirror with 50 nm Pt-coating
Radius	14 km
Distance from source	21 200 mm
Incidence angle	3 mrad
Active length	1200 mm
Monochromator	
Distance from source	24 100 mm
Energy range	7.5–36 keV
Energy resolution ($\Delta E/E$)	1.4×10^{-4} [Si (111)]
Focusing mirror	
Tangential radius	8.9 km
Sagittal radius	50 mm
Distance from source	27 000 mm
Incidence angle	3 mrad
Active length	1200 mm

2.1.2. Beamline optical layout

The main optical components (Table 1, Fig. 3) found along the beamline are a platinum-coated vertical collimating mirror and a platinum-coated vertical-bendable toroidal focusing mirror positioned, respectively, before and after a fixed-exit, cryogenic (LN₂) double-crystal Si(111) monochromator in

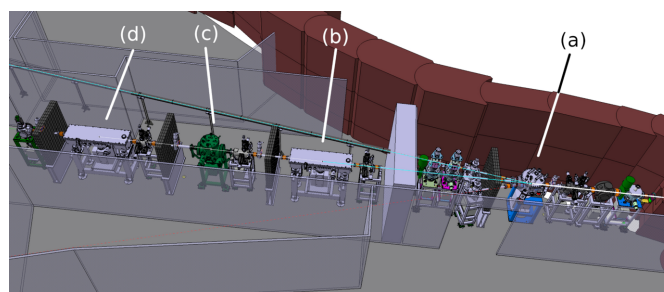


Figure 3

Main elements of the present XRD2 beamline at Elettra. Super-conductive source on the right: (a) beam splitter, feeding Xpress and HF-SAXS beamlines (the latter not shown) in addition to the central XRD2; (b) collimating mirror; (c) monochromator and (d) focusing mirror.

non-dispersive configuration. The latter is an in-house development (Gambitta, 2010), with the capability to deliver a monochromatic beam in the range 7.5–36 keV (usually limited to 8–20 keV for MX measurements) with the Si(111) bandwidth resolution. Most of the data collections are performed at wavelengths around 1.0 Å. The beam position and intensity at the experiment are measured using a four-quadrant beam position monitor (Alibava Systems) and stabilized/optimized via a feedback system acting on the optical components.

The measured size of the focal spot and the relative angular divergences confirm the expected values, $290\text{ }\mu\text{m} \times 90\text{ }\mu\text{m}$ (FWHM) and $2.0\text{ mrad} \times 0.25\text{ mrad}$ (FWHM), respectively, with a native full flux of $1.7 \times 10^{12}\text{ photons s}^{-1}$ at 1 Å. With a typical aperture of $100\text{ }\mu\text{m}$ the flux would be $\sim 6 \times 10^{11}\text{ photons s}^{-1}$. A typical data collection at XRD2 on a $100\text{ }\mu\text{m} \times 100\text{ }\mu\text{m} \times 100\text{ }\mu\text{m}$ crystal would result in an average diffraction weighted dose of 5.6 MGy, as calculated using *RADDOSE-3D* software (Zeldin *et al.*, 2013), which is within the Garman limit (Owen *et al.*, 2006).

2.1.3. Experimental station

The main components of the end-station are an MD2-S diffractometer (Arinax) combined with a large-area Pilatus 6M detector (Dectris) with a sensor thickness of 320 mm and a maximum readout rate of 12 Hz (Fig. 1). A set of round apertures of sizes 20, 50, 75, 100 and $150\text{ }\mu\text{m}$ allows one to adapt the size of the beam to the samples. Apertures are followed by a clean-up capillary extending to the crystalline sample to reduce the image background. A set of attenuators can be used to reduce the beam intensity if the sample(s) are expected to undergo radiation damage. The standard acquisition time is about 1 s per degree or 6 min for a full sphere with unattenuated beam and aperture of $100\text{ }\mu\text{m}$, allowing daily data collections of samples contained in ten pucks.

Ancillary equipment includes a fluorescence detector (X123 SDD from Amptek) used for beamline calibration, for very rare MAD measurements or for the identification of an (unexpected) bound heavy atom. The setup allows also one to anneal the sample to enhance its crystalline order via the control interface. The automounter offers a storage dewar hosting up to 192 SPINE-compliant samples based on UNIPUCKS-type pucks. Its open-lid configuration provides quick access and easy insertion and removal of pucks. The integration between the robotic arm (Stäubli TXL-60), dewar and diffractometer was developed in-house. Automatic reading/checking of the pin data matrix is available and is encouraged. The IRELEC double gripper minimizes the duty cycle between samples to $\sim 40\text{ s}$, which remains negligible compared with typical data collection times, and allows a full shipping canister screening in less than 4 h.

2.2. The general purpose X-ray diffraction XRD1 beamline

The X-Ray Diffraction 1 (XRD1) beamline has been designed – in collaboration with the Istituto di Cristallografia, CNR – to perform a wide variety of measurements and experiments, all based on diffraction (Lausi *et al.*, 2015). The

beamline exploits a 4.5 m wiggler as source of radiation and is equipped with a collimating mirror and a toroidal focusing one, together with a cryogenically cooled (LN_2), Si(111) double-crystal, fixed-exit monochromator. The latter provides a monochromatic beam in the wide energy range of 4–21.5 keV.

The flux at the sample is in the range $10^{12}\text{ photons s}^{-1}$, with a natural beam footprint of $700\text{ }\mu\text{m}$ (H) \times $200\text{ }\mu\text{m}$ (V) reduced via a set of round apertures of sizes 200, 100, 50, 20 and $5\text{ }\mu\text{m}$. Key equipment includes a hybrid pixel area detector (Pilatus 2M from Dectris) and a versatile setup including a κ -geometry goniostat and a robotic arm for handling different samples, hosting single crystals, powders, and thin films in fields ranging from macromolecular crystallography to materials science, under normal, extreme, and special conditions (Polentarutti *et al.*, 2004).

The availability of longer wavelengths allows us to offer to the MX community the opportunity to exploit the enhancement of anomalous signal from biologically relevant elements such as sulfur, phosphorus, chlorine and calcium (Mueller-Dieckmann *et al.*, 2004; Weiss *et al.*, 2004; Djinojic Carugo *et al.*, 2005; Mueller-Dieckmann *et al.*, 2005). Thus, for MX, XRD1 complements XRD2 data collection at longer wavelengths, upon user request, with the option to use a helium purged beam path to mitigate the effects of air scatter (Polentarutti *et al.*, 2004).

3. XRD2 and XRD1 software, computing and data policy

Macromolecular crystallography is a mature field where facilities have invested in dedicated and standardized beamlines while dedicated software, such as *autoPROC* (Vonrhein *et al.*, 2011), *XDS* (Kabsch, 2010), *CCP4* (Agirre *et al.*, 2023) and so on, have streamlined the ever growing needs for guided data collection and fast data analysis. At Elettra, low-level controls are based on the TANGO system control framework (<https://www.tango-controls.org/>), combined with Python scripting to handle complex functions or build up control interfaces. High-level web interfaces dedicated to data collection, both local and remote, like *MXCuBE3* (Mueller *et al.*, 2017) and *Braggy* (ESRF, <https://gitlab.esrf.fr/ui/h5web-braggy>), have been installed and further developed together with the MX software community. They have been made available to MX users, together with automatic pipelines for online data analysis and re-analysis (the latter at the moment on demand only). To help users to make faster and better decisions, *DISTL* (Zhang *et al.*, 2006) is run as the data collection is progressing to provide a preliminary evaluation of data, *autoPROC* (Vonrhein *et al.*, 2011) and *fastDP* (Winter & McAuley, 2011) provide quick metrics for space group, symmetry and results of integration of the data, while *DIMPLE* (<https://ccp4.github.io/dimple/>) generates electron density maps with focus on interesting electron density blobs. Data analysis is performed on the Elettra High Performance Computing Cluster. Typical data analysis times are comparable with standard data collection durations, enabling users to

incorporate prior sample characterization effectively into their decision-making process. MX data and metadata are archived via *ISPyB* (Delagenière *et al.*, 2011), paired with the *SynchWeb* frontend (Fisher *et al.*, 2015) and integrated within Elettra's user portal.

Elettra's data policy adheres to the FAIR principles — Findability, Accessibility, Interoperability and Reusability — ensuring that all research data generated at the facility are organized, accessible and useful for the scientific community. This policy mandates that all data are stored with comprehensive metadata, facilitating easy discovery and retrieval. By implementing standardized formats, Elettra promotes interoperability, allowing data integration across diverse scientific disciplines. Additionally, data are shared under clear usage terms, fostering reuse while protecting intellectual property rights. Through this FAIR-compliant approach, Elettra supports open science, advancing innovation and collaboration across global research communities.

4. Access mode to MX beamlines

Elettra adopted a monthly based proposal submission system to accommodate the needs for fast access to XRD2. All new proposals for individual research groups are sent to the review panel upon submission, and time is allocated at the beginning of the following month. This creates an agile scheduling which fills up the calendar only a week or so in advance by scheduling users when they are ready and eager to collect on freshly produced samples. The scheduling is confirmed when the dewar arrives and easy rescheduling can be done if some delays occur during shipping. Multiple visits can be associated with each proposal, and the scheduling windows are by the hour rather than the usual 8 h shifts.

In order to gain access to *MXCuBE*, the proposal has to be scheduled via the Elettra Virtual Unified Office portal (VUO, <https://vuo.elettra.eu>), so that users associated with a specific proposal can connect and collect/analyse data using their own VUO credentials.

5. Associated facilities for structural biology

A Structural Biology laboratory (SBlab) was established at Elettra with the aim of supporting the MX beamlines and to carry out in-house research, with projects including cancer biology, neurodegenerative diseases, and bacterial and viral infections. In addition to in-house research, SBlab caters to external users via a crystallization and a protein-production facility, which have recently undergone a significant upgrade funded through the NextGenerationEU PRP@CERIC project (<https://www.pathogen-ri.eu/>).

The protein-production facility is equipped to handle the entire workflow, from gene to protein structure. The crystallization facility includes a MosquitoX3 (TTP-Labtech) equipped with an anti-evaporation chamber, for setting up sitting-drop crystallization trials in 96-well microplates; to support high-throughput monitoring, two Formulatrix Rock Imager 360 systems with UV, VIS and MFI optics have been

acquired — one will operate at room temperature and the other at 4°C. These instruments will enable fully automated crystallization processes. The associated software allows users to remotely monitor crystallization experiments in real time.

A new CryoEM facility is being established at the neighbouring CNR Istituto Officina dei Materiali (IOM), and will be jointly managed by IOM and Elettra, providing further structural biology opportunities to the Elettra user community. The facility will include a Glacios2 Cryo-TEM equipped with a Falcon 4 direct electron detector and Selectris energy filter (ThermoFisher Scientific) as well as an Aquilos2 Cryo-FIB/SEM (ThermoFisher Scientific) for the preparation of thin cryo-lamellae. The facility will therefore be able to cover the whole range of electron-based techniques, from single-particle CryoEM analysis, to cryo-electron tomography (CryoET) from biological organelles or frozen cellular lamellas, to electron diffraction on sub-micrometric crystals (MicroED), thus ideally complementing the X-ray diffraction structural biology techniques available at Elettra.

6. In-house research

Currently, SBlab hosts the Protein Targets for Drug Discovery group, and the DNA Replication and Repair group. The Protein Targets for Drug Discovery group, investigating structural properties of druggable proteins to support structure-based drug design, was an active player in the concerted effort to explore solutions to treat COVID-19, as participant in the EU EXSCALATE4CoV project (<https://www.exscalate4cov.eu/>), led by the Italian Pharmaceutical company Dompé, and involving 18 teams from seven EU countries to identify potential compounds binding to viral targets. As a result, 29 structures were deposited in the Protein Data Bank and six publications involved the contribution of XRD2 (Kuzikov *et al.*, 2021; Pelliccia *et al.*, 2022; Stefanelli *et al.*, 2023; Gossen *et al.*, 2021; Costanzi *et al.*, 2021; Albani *et al.*, 2024). This initial effort spun new collaboration opportunities such as a new Horizon Europe project, named AVITHRAPID (Antiviral Therapeutics for Rapid Response Against Pandemic Infectious Diseases, <https://avithrapid.eu/>).

The DNA Replication and Repair group has long-standing experience in applying molecular and structural biology tools to study the basic genetic processes within the cell, such as DNA replication and repair, using crystallography, electron microscopy, and small-angle X-ray scattering. As genomic instability, which could result from errors in DNA replication and repair, is closely connected with tumour development, this research has been funded over the years by the Italian Association for Cancer Research (AIRC), various INTERREG projects (PROTEO, GLIOMA, TRANS-GLIOMA) and the Marie Curie MSCA network AntiHelix (<https://www.elettra.eu/AntiHelix/>), aimed at finding inhibitors leading to novel anti-tumour drugs. Most projects focused on the role of helicases in proliferation and genome stability, involving proteins such as the replicative MCM helicase complex and associated factors forming the CMG complex, the PCNA ring (De March *et al.*, 2017; De March *et al.*, 2018;

Gonzalez-Magaña *et al.*, 2019), and the FeS helicases DDX11 (Bottega *et al.*, 2021), FANCI (Boavida *et al.*, 2024), RTEL1 (Cortone *et al.*, 2024), and DinG (De Pianta *et al.*, 2023).

7. Highlights from the MX crystallography beamlines

The Elettra MX user community includes several academic and industrial groups from Italy and neighbouring countries, together with a large community of Indian groups supported by the XRD2 Indian partner. The span of their activities is from novel structures to structure-based drug discovery projects. Several high-impact MX publications have appeared from the two beamlines.

Worth noting from XRD1 beamline are the crystal structure of the lysenin pore (Podobnik *et al.*, 2016), the crystal structures of *Arabidopsis* and *Chlamydomonas* phosphoribulokinase (Gurrieri *et al.*, 2019) and the structure of human *N*-acylphosphatidylethanolamine-hydrolyzing phospholipase D (Magotti *et al.*, 2015).

Highlights from the XRD2 beamline include a number of *de novo* structures, such as the complex between Uba4 (ubiquitin-like protein activator 4) and Urm1 (ubiquitin-related modifier 1), responsible for the synthesis of 2-thiolated wobble uridine (U₃₄) in tRNA (Pabis *et al.*, 2020), the molecular architecture of the glycogen-committed PP1/PTG holoenzyme combining MX and SAXS analysis (Semrau *et al.*, 2022), and an integrated structural analysis of the C-terminal domain of the RTEL1 helicase (Cortone *et al.*, 2024).

A large part of the users' community of XRD2 is involved in structure-based drug design projects, against targets such as carbonic anhydrase (implicated in glaucoma, epilepsy, cancer, and osteoporosis). An example is the structure of human carbonic anhydrase II in a complex with a carbonic anhydrase/telomerase dual-hybrid inhibitor (Berrino *et al.*, 2020). Among the inhibitors of other molecular targets, we wish to highlight the structure of thrombin with a G4-based aptamer with improved anti-coagulant properties (Troisi *et al.*, 2023), the structure of cathepsin K with a covalently bound alkyne inhibitor (Mons *et al.*, 2019), the inhibition of urease with mono- and di-substituted catechols (Mazzei *et al.*, 2021), and the molecular basis of the interaction between monoclonal antibodies and oligosaccharides involved in *Neisseria meningitidis* infections (Pietri *et al.*, 2024).

The Indo-Italian partnership for XRD2 has been productive, resulting in high impact publications, such as: the high resolution (~ 1 Å) crystal structure of the complex of Fyn kinase SH3 domain with Tau protein, with implications in Alzheimer's disease (Jos *et al.*, 2024); the crystal structure of the complex between DarT toxin and DarG antitoxin from *Mycobacterium tuberculosis* (Deep *et al.*, 2023); structural studies of neurotransmitter-inhibitor complexes implicated in pain and epilepsy therapies (Joseph *et al.*, 2022, Pidathala *et al.*, 2021); structure based drug design with SARS-COV2 (Panchariya *et al.*, 2021); and the crystal structure of the Y-family DNA polymerase from *Mycobacterium smegmatis* (Johnson *et al.*, 2019).

8. A vision for macromolecular crystallography at Elettra 2.0

In early 2023, Elettra conducted an informal survey to assess the current and future needs of its academic and industrial structural biology community. The results of the survey indicated that the majority of users opt for standard native MX data collection, especially for ligand screening, with some use of SAD phasing, and of advanced techniques like *in situ* plate screening, serial data collection and time-resolved MX. However, users anticipate a shift towards more diverse data collection methods in the future, with even greater interest in ligand screening, *in situ* plate screening and the integration of MX with spectroscopy.

At present, most users utilize a $50\text{ }\mu\text{m} \times 50\text{ }\mu\text{m}$ beam, although there is a growing trend toward smaller $5\text{ }\mu\text{m} \times 5\text{ }\mu\text{m}$ beams. Users have expressed interest in a κ -goniostat, as well as hardware and software for mesh scanning and fragment screening. Current microfocus beamlines, together with new crystal handling methods and the implementation of novel data processing approaches, allow one to obtain high resolution X-ray data also from crystals smaller than $5\text{ }\mu\text{m}$. Such crystal size limits can be found with large macromolecular complexes, membrane proteins, or proteins with unstructured regions or viral particles, where the optimization of the crystallization kinetics and thermodynamics to increase the size of the crystals was not successful. In addition to traditional microcrystals obtained from purified proteins using standard batch crystallization techniques, a growing and very interesting area of application is the structural analysis of *in vivo* assembled viral superstructures (Coulibaly, 2019) or *in cellulo* crystallized recombinant protein (Schönherr *et al.*, 2024). To address these challenges and meet the future demands of structural biology, a new beamline for MX is being developed as part of the Elettra 2.0 upgrade to a fourth-generation light source. As part of this upgrade, which promises a significant increase in brightness (approximately 35 times at 1 keV and 160 times at 10 keV), the XRD2 beamline will be replaced with a new beamline.

The new MX beamline, called μ XRD, will be based on an in-vacuum undulator source, generating a low divergence, high brilliance beam (Fig. 4). The designed optical scheme (Fig. 5) foresees a cryogenic double crystal monochromator working in the range 5–17 keV and a focusing optical element based on a Kirkpatrick–Baez configuration. The monochromator will be able to work in a high resolution mode – based on Si(111) crystals – and in a high flux mode – based on a couple of multilayer mirrors having a bandwidth of $\sim 1\%$ and expected to guarantee an increase of an order of magnitude in flux.

The expected flux at the sample in high resolution mode is $\sim 5 \times 10^{12}$ photons s^{-1} within a spot size of $5\text{ }\mu\text{m} \times 5\text{ }\mu\text{m}$ (FWHM), quickly expandable up to $50\text{ }\mu\text{m} \times 50\text{ }\mu\text{m}$ (Fig. 6) and beyond. The beamline will therefore be able to host small samples and offer the possibility to screen/scan larger ones, collect complete datasets faster, handle radiation damage better, and enable serial synchrotron crystallography experi-

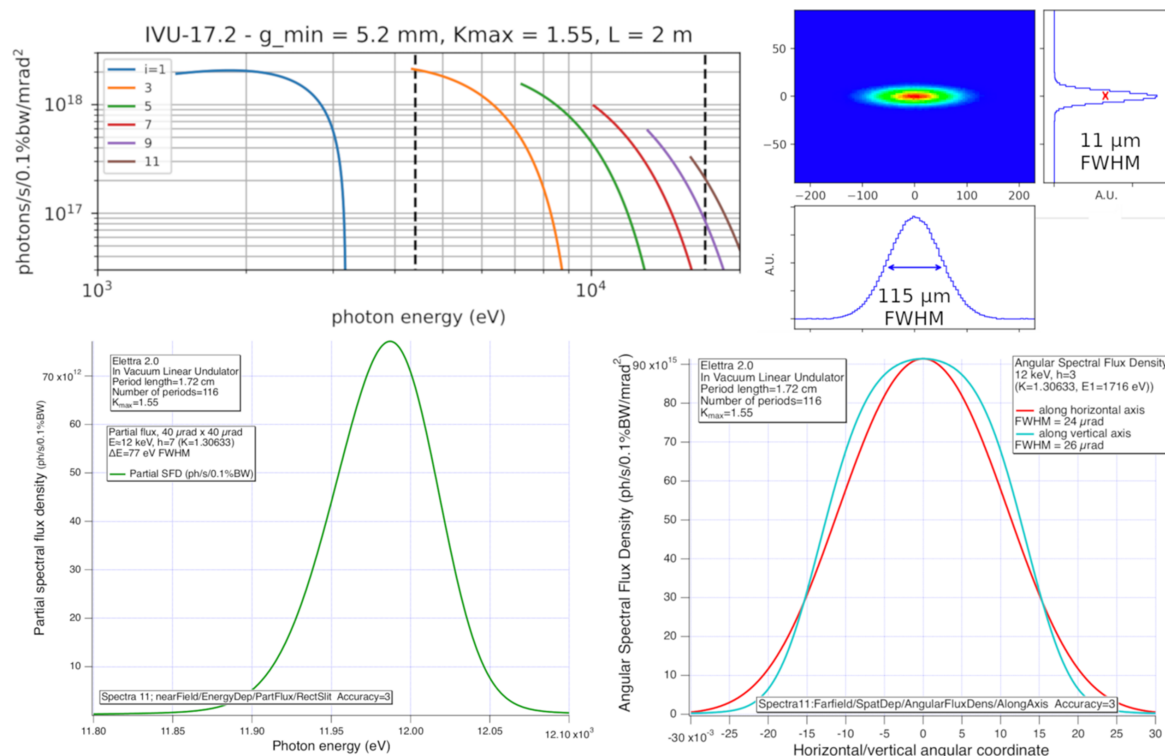


Figure 4

Expected performance of the μ XRD in-vacuum undulator (period 17.2 mm, minimum gap 5.2 mm, 116 periods, $K_{\max} = 1.55$, Elettra 2.0 parameters, 2.4 GeV, 400 mA). From top-left clockwise: spectral flux, showing odd harmonics; spatial photon beam size at 12 keV, $h = 7$; angular photon beam size at 12 keV, $h = 7$; partial $40 \mu\text{rad} \times 40 \mu\text{rad}$ spectral flux density showing the energy line width at the monochromator.

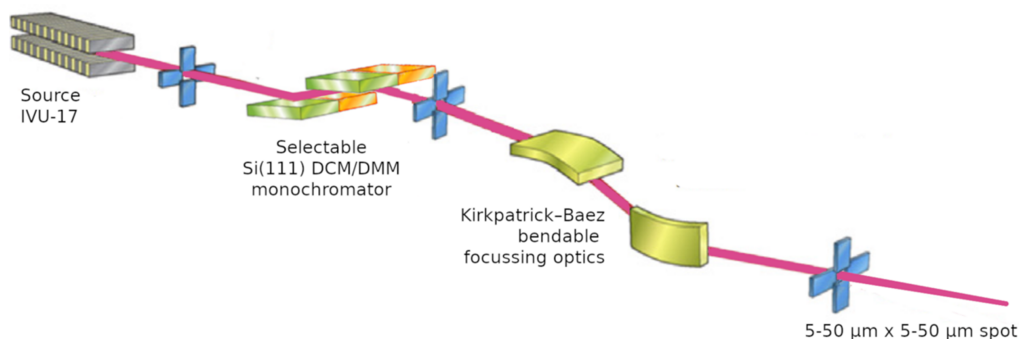


Figure 5

Optical scheme of the μ XRD beamline at Elettra 2.0.

ments on fixed targets, including at room temperature. Together with the newly upgraded crystallization facility, it will provide a state-of-the-art platform for high-throughput crystallization and structure-based drug discovery. The planned experimental setup includes a fast, large-area detector, auto-mounter and multi-axis goniometry, coupled with an infrastructure control software and pipelines for automated data collection, processing, evaluation and interpretation, aided by the incoming artificial intelligence. The μ XRD beamline is due to come into operation in 2027.

9. Conclusions

Macromolecular X-ray crystallography represents a cornerstone of user operations at the Elettra Synchrotron, attracting a diverse community of researchers from across Europe and

beyond. The XRD2 beamline, dedicated to MX measurements, provides a high photon flux and integrates advanced hardware and software automation within user-friendly, web-based interfaces.

As part of Elettra's upgrade to a diffraction-limited machine, XRD2 will be replaced by μ XRD, a next-generation beamline offering significantly enhanced brilliance. This advancement is set to unlock new possibilities for studying challenging samples and employing innovative data-collection methods.

To complement both current and future MX beamlines, Elettra has strategically implemented supporting facilities, including protein production and crystallization laboratories. These are being further strengthened with the addition of a state-of-the-art cryo-electron microscopy facility, ensuring a comprehensive infrastructure for structural biology research.

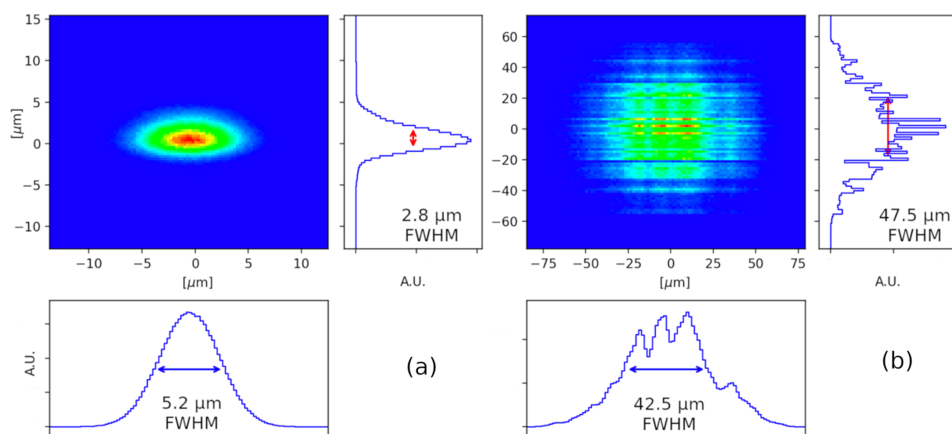


Figure 6

Ray tracing simulations based on Elettra 2.0 phase 2 machine parameters for the μ XRD beam spot at the sample position using *DABAM/ShadowOui* simulated profiles (slope error of 0.15 μ rad and 0.3 μ rad for the vertical and horizontal focusing mirror, respectively) show the possibility to reach (a) the expected final beam size of 5 μ m \times 5 μ m, expandable to (b) 50 μ m \times 50 μ m.

Acknowledgements

The authors express their gratitude to all Elettra staff members involved in the design, construction and commissioning of the XRD2 beamline. Special recognition is given to the IT group for their work on the new web-based control interfaces. The authors also acknowledge the invaluable contributions of all Elettra working groups supporting the design and implementation of the incoming Elettra 2.0 project, with particular appreciation for the work performed by the Accelerators and Optics groups on the forthcoming μ XRD beamline. Dr Shekhar C. Mande, Savitribai Phule Pune University, Pune, India, and Dr S. M. Sharma, Bhabha Atomic Research Centre, Mumbai, India, are gratefully acknowledged for their contributions in the early stages of planning and assembly of the XRD2 project. RPH and NKV acknowledge the International Centre for Theoretical Physics (ICTP), Trieste, Italy, and the Indian Institute of Science, Bengaluru, India, for the IISc-ICTP fellowships. The Elettra 2.0 project is supported by Italian national funds through the Fondo per il Finanziamento degli Investimenti e lo Sviluppo Infrastrutturale del Paese, established by the 2017 Budget Law (Article 1, Paragraph 140, of Law No. 232/2016). The XRD2 beamline has been co-funded by Elettra and the Department of Science and Technology, Ministry of Science and Technology, Government of India, and is currently operated in collaboration with the Indian Institute of Science, Bengaluru, India. The structural biology laboratory upgrades are supported by the CERIC-ERIC Internal Research Grant INTEGRA and by the European NextGenerationEU program, through the Pathogen Readiness Platform for CERIC-ERIC Upgrade project (PRP@CERIC, <https://www.pathogen-ri.eu/>), which supports both enhanced crystallization and protein characterization facilities, as well as the establishment of the CryoEM facility, the latter in collaboration with the Istituto Officina dei Materiali (IOM), part of the National Research Council of Italy (Consiglio Nazionale delle Ricerche, CNR). Open access publishing facilitated by Elettra Sincrotrone Trieste ScpA, as part of the Wiley – CRUI-CARE agreement.

References

- Agirre, J., Atanasova, M., Bagdonas, H., Ballard, C. B., Baslé, A., Beilstein-Edmands, J., Borges, R. J., Brown, D. G., Burgos-Mármol, J. J., Berrisford, J. M., Bond, P. S., Caballero, I., Catapano, L., Chojnowski, G., Cook, A. G., Cowtan, K. D., Croll, T. I., Debreczeni, J. É., Devenish, N. E., Dodson, E. J., Drevon, T. R., Emsley, P., Evans, G., Evans, P. R., Fando, M., Foadi, J., Fuentes-Montero, L., Garman, E. F., Gerstel, M., Gildea, R. J., Hatti, K., Hekkelman, M. L., Heuser, P., Hoh, S. W., Hough, M. A., Jenkins, H. T., Jiménez, E., Joosten, R. P., Keegan, R. M., Keep, N., Krissinel, E. B., Kolenko, P., Kovalevskiy, O., Lamzin, V. S., Lawson, D. M., Lebedev, A. A., Leslie, A. G. W., Lohkamp, B., Long, F., Malý, M., McCoy, A. J., McNicholas, S. J., Medina, A., Millán, C., Murray, J. W., Murshudov, G. N., Nicholls, R. A., Noble, M. E. M., Oeffner, R., Pannu, N. S., Parkhurst, J. M., Pearce, N., Pereira, J., Perrakis, A., Powell, H. R., Read, R. J., Rigden, D. J., Rochira, W., Sammito, M., Sánchez Rodríguez, F., Sheldrick, G. M., Shelley, K. L., Simkovic, F., Simpkin, A. J., Skubak, P., Sobolev, E., Steiner, R. A., Stevenson, K., Tews, I., Thomas, J. M. H., Thorn, A., Valls, J. T., Uski, V., Usón, I., Vagin, A., Velankar, S., Vollmar, M., Walden, H., Waterman, D., Wilson, K. S., Winn, M. D., Winter, G., Wojdyr, M. & Yamashita, K. (2023). *Acta Cryst.* **D79**, 449–461.
- Albani, S., Costanzi, E., Hoang, G. L., Kuzikov, M., Frings, M., Ansari, N., Demitri, N., Nguyen, T. T., Rizzi, V., Schulz, J. B., Bolm, C., Zaliani, A., Carloni, P., Storici, P. & Rossetti, G. (2024). *J. Chem. Inf. Model.* **64**, 892–904.
- Berrino, E., Angeli, A., Zhdanov, D. D., Kiryukhina, A. P., Milaneschi, A., De Luca, A., Bozdog, M., Carradori, S., Sella, S., Bartolucci, G., Peat, T. S., Ferraroni, M., Supuran, C. T. & Carta, F. (2020). *J. Med. Chem.* **63**, 7392–7409.
- Boavida, A., Napolitano, L. M., Santos, D., Cortone, G., Jegadesan, N. K., Onesti, S., Branzai, D. & Pisani, F. M. (2024). *EMBO Rep.* **25**, 876–901.
- Bottega, R., Ravera, S., Napolitano, L. M. R., Chiappetta, V., Zini, N., Crescenzi, B., Arniani, S., Faleschini, M., Cortone, G., Faletta, F., Medagli, B., Sirchia, F., Moretti, M., de Lange, J., Cappelli, E., Mecucci, C., Onesti, S., Pisani, F. M. & Savoia, A. (2021). *J. Cell. Physiol.* **236**, 5664–5675.
- Cortone, G., Graewert, M. A., Kanade, M., Longo, A., Hegde, R., González-Magaña, A., Chaves-Arquero, B., Blanco, F. J., Napolitano, L. M. R. & Onesti, S. (2024). *Protein Sci.* **33**, e5093.
- Costanzi, E., Kuzikov, M., Esposito, F., Albani, S., Demitri, N., Giabbai, B., Camasta, M., Tramontano, E., Rossetti, G., Zaliani, A. & Storici, P. (2021). *Int. J. Mol. Sci.* **22**, 11779.
- Coulbaly, F. (2019). *Advances in Virus Research*, edited by F. A. Rey, pp. 275–335. Academic Press.

- Deep, A., Singh, L., Kaur, J., Velusamy, M., Bhardwaj, P., Singh, R. & Thakur, K. G. (2023). *Structure*, **31**, 780–789.e4.
- Delagenière, S., Brenchereau, P., Launer, L., Ashton, A. W., Leal, R., Veyrier, S., Gabadinho, J., Gordon, E. J., Jones, S. D., Levik, K. E., McSweeney, S. M., Monaco, S., Nanao, M., Spruce, D., Svensson, O., Walsh, M. A. & Leonard, G. A. (2011). *Bioinformatics*, **27**, 3186–3192.
- De March, M., Barrera-Vilarmau, S., Crespan, E., Mentegari, E., Merino, N., Gonzalez-Magaña, A., Romano-Moreno, M., Maga, G., Crehuet, R., Onesti, S., Blanco, F. J. & De Biasio, A. (2018). *Nucleic Acids Res.* **46**, 9816–9828.
- De March, M., Merino, N., Barrera-Vilarmau, S., Crehuet, R., Onesti, S., Blanco, F. J. & De Biasio, A. (2017). *Nat. Commun.* **8**, 13935.
- De Piante, E., D'Aria, F., Napolitano, L. M. R., Amato, J., Pirrello, S., Onesti, S. & Giancola, C. (2023). *Sci. Rep.* **13**, 12610.
- Djinović Carugo, K., Helliwell, J. R., Stuhmann, H. & Weiss, M. S. (2005). *J. Synchrotron Rad.* **12**, 410–419.
- Fisher, S. J., Levik, K. E., Williams, M. A., Ashton, A. W. & McAuley, K. E. (2015). *J. Appl. Cryst.* **48**, 927–932.
- Franciosi, A. & Kiskinova, M. (2023). *Eur. Phys. J. Plus*, **138**, 79.
- Gambitta, A. (2010). *Diamond Light Source Proc.* **1**, e23.
- Gonzalez-Magaña, A., Ibáñez de Opakua, A., Romano-Moreno, M., Murciano-Calles, J., Merino, N., Luque, I., Rojas, A. L., Onesti, S., Blanco, F. J. & De Biasio, A. (2019). *J. Biol. Chem.* **294**, 3947–3956.
- Gossen, J., Albani, S., Hanke, A., Joseph, B. P., Bergh, C., Kuzikov, M., Costanzi, E., Manelfi, C., Storici, P., Gribbon, P., Beccari, A. R., Talarico, C., Spyraakis, F., Lindahl, E., Zaliani, A., Carloni, P., Wade, R. C., Musiani, F., Kokh, D. B. & Rossetti, G. (2021). *ACS Pharmacol. Transl. Sci.* **4**, 1079–1095.
- Gregoratti, L., Lizzit, S., Karantzoulis, E. & Franciosi, A. (2024). *Synchrotron Radiat. News* **37**(1), 39–44.
- Gurrieri, L., Del Giudice, A., Demitri, N., Falini, G., Pavel, N. V., Zaffagnini, M., Polentarutti, M., Crozet, P., Marchand, C. H., Henri, J., Trost, P., Lemaire, S. D., Sparla, F. & Fermani, S. (2019). *Proc. Natl Acad. Sci. USA*, **116**, 8048–8053.
- Johnson, M. K., Kottur, J. & Nair, D. T. (2019). *Nucleic Acids Res.* **47**, 10693–10705.
- Jos, S., Poulouse, R., Kambaru, A., Gogoi, H., Dalavaikodihalli Nanjaiah, N., Padmanabhan, B., Mehta, B. & Padavattan, S. (2024). *J. Mol. Biol.* **436**, 168445.
- Joseph, D., Nayak, S. R. & Penmatsa, A. (2022). *EMBO J.* **41**, e110735.
- Kabsch, W. (2010). *Acta Cryst. D* **66**, 125–132.
- Karantzoulis, E., Di Mitri, S., Barbo, F., Barletta, W., Bassanese, S., Bracco, R., Brajnik, G., Buonanno, A., Caiazza, D., Carniel, A., Castronovo, D., Cautero, M., Cleva, S., Comisso, M., Cudin, I., Dastan, S., De Monte, R., Diviacco, B., Fabris, A., Fabris, R., Gaio, G., Grulja, S., Gregoratti, L., Gubertini, A., Krecic, S., Lizzit, S., Loda, G., Lonza, M., Manukyan, K., Mazzucco, B., Milani, M., Millo, D., Modica, M., Novinec, L., Pangon, G., Pasotti, C., Passarelli, A., Rumiz, L., Sbarra, S., Scrimali, G., Shafqat, N., Simonetti, G., Svandrik, M., Tripaldi, F., Veronese, M., Visintini, R., Yousefi, E. & Zaccaria, M. (2024). *Nucl. Instrum. Methods Phys. Res. A*, **1060**, 169007.
- Kuzikov, M., Costanzi, E., Reinshagen, J., Esposito, F., Vangeel, L., Wolf, M., Ellinger, B., Claussen, C., Geisslinger, G., Corona, A., Iaconis, D., Talarico, C., Manelfi, C., Cannalire, R., Rossetti, G., Gossen, J., Albani, S., Musiani, F., Herzog, K., Ye, Y., Giabbai, B., Demitri, N., Jochmans, D., Jonghe, S. D., Rymenants, J., Summa, V., Tramontano, E., Beccari, A. R., Leyssen, P., Storici, P., Neyts, J., Gribbon, P. & Zaliani, A. (2021). *Am. Chem. Soc. Pharmacol. Transl. Sci.* **4**, 1096–1110.
- Lausi, A., Polentarutti, M., Onesti, S., Plaisier, J. R., Busetto, E., Bais, G., Barba, L., Cassetta, A., Campi, G., Lamba, D., Pifferi, A., Mande, S. C., Sarma, D. D., Sharma, S. M. & Paolucci, G. (2015). *Eur. Phys. J. Plus*, **130**, 43.
- Magotti, P., Bauer, I., Igarashi, M., Babagoli, M., Marotta, R., Piomelli, D. & Garau, G. (2015). *Structure*, **23**, 598–604.
- Mazzei, L., Contaldo, U., Musiani, F., Cianci, M., Bagnolini, G., Roberti, M. & Ciarli, S. (2021). *Angew. Chem. Int. Ed.* **60**, 6029–6035.
- Mons, E., Jansen, I. D. C., Loboda, J., van Doodewaerd, B. R., Hermans, J., Verdoes, M., van Boeckel, C. A. A., van Veelen, P. A., Turk, B., Turk, D. & Ovaa, H. (2019). *J. Am. Chem. Soc.* **141**, 3507–3514.
- Mueller, U., Thunnissen, M., Nan, J., Eguiraun, M., Bolmsten, F., Milán-Otero, A., Guijarro, M., Oscarsson, M., de Sanctis, D. & Leonard, G. (2017). *Synchrotron Radiat. News* **30**(1), 22–27.
- Mueller-Dieckmann, C., Panjikar, S., Tucker, P. A. & Weiss, M. S. (2005). *Acta Cryst. D* **61**, 1263–1272.
- Mueller-Dieckmann, C., Polentarutti, M., Djinovic Carugo, K., Panjikar, S., Tucker, P. A. & Weiss, M. S. (2004). *Acta Cryst. D* **60**, 28–38.
- Owen, R. L., Rudiño-Piñera, E. & Garman, E. F. (2006). *Proc. Natl Acad. Sci. USA*, **103**, 4912–4917.
- Pabis, M., Termathe, M., Ravichandran, K. E., Kienast, S. D., Krutyholowa, R., Sokolowski, M., Jankowska, U., Grudnik, P., Leidel, S. A. & Glatt, S. (2020). *EMBO J.* **39**, e105087.
- Panchariya, L., Khan, W. A., Kuila, S., Sonkar, K., Sahoo, S., Ghoshal, A., Kumar, A., Verma, D. K., Hasan, A., Khan, M. A., Jain, N., Mohapatra, A. K., Das, S., Thakur, J. K., Maiti, S., Nanda, R. K., Halder, R., Sunil, S. & Arockiasamy, A. (2021). *Chem. Commun.* **57**, 10083–10086.
- Pelliccia, S., Cerchia, C., Esposito, F., Cannalire, R., Corona, A., Costanzi, E., Kuzikov, M., Gribbon, P., Zaliani, A., Brindisi, M., Storici, P., Tramontano, E. & Summa, V. (2022). *Eur. J. Med. Chem.* **244**, 114853.
- Pidathala, S., Mallela, A. K., Joseph, D. & Penmatsa, A. (2021). *Nat. Commun.* **12**, 2199.
- Pietri, G. P., Bertuzzi, S., Karnicar, K., Unione, L., Lisnic, B., Malic, S., Miklic, K., Novak, M., Calloni, I., Santini, L., Usenik, A., Romano, M. R., Adamo, R., Jonjic, S., Turk, D., Jiménez-Barbero, J. & Lenac Rovis, T. (2024). *Carbohydr. Polym.* **341**, 122349.
- Podobnik, M., Savory, P., Rojko, N., Kisovec, M., Wood, N., Hambley, R., Pugh, J., Wallace, E. J., McNeill, L., Bruce, M., Liko, I., Allison, T. M., Mehmood, S., Yilmaz, N., Kobayashi, T., Gilbert, R. J. C., Robinson, C. V., Jayasinghe, L. & Anderluh, G. (2016). *Nat. Commun.* **7**, 11598.
- Polentarutti, M., Glazer, R. & Djinović Carugo, K. (2004). *J. Appl. Cryst.* **37**, 319–324.
- Schönherr, R., Boger, J., Lahey-Rudolph, J. M., Harms, M., Kaiser, J., Nachtschatt, S., Wobbe, M., Duden, R., König, P., Bourenkov, G., Schneider, T. R. & Redecke, L. (2024). *Nat. Commun.* **15**, 1709.
- Semrau, M. S., Giachin, G., Covaceuszach, S., Cassetta, A., Demitri, N., Storici, P. & Lolli, G. (2022). *Nat. Commun.* **13**, 6199.
- Stefanelli, I., Corona, A., Cerchia, C., Cassese, E., Improta, S., Costanzi, E., Pelliccia, S., Morasso, S., Esposito, F., Paulis, A., Scognamiglio, S., Di Leva, F. S., Storici, P., Brindisi, M., Tramontano, E., Cannalire, R. & Summa, V. (2023). *Eur. J. Med. Chem.* **253**, 115311.
- Troisi, R., Napolitano, V., Rossitto, E., Osman, W., Nagano, M., Wakui, K., Popowicz, G. M., Yoshimoto, K. & Sica, F. (2023). *Nucleic Acids Res.* **51**, 8880–8890.
- Vonrhein, C., Flensburg, C., Keller, P., Sharff, A., Smart, O., Paciorek, W., Womack, T. & Bricogne, G. (2011). *Acta Cryst. D* **67**, 293–302.
- Weiss, M. S., Mander, G., Hedderich, R., Diederichs, K., Ermler, U. & Warkentin, E. (2004). *Acta Cryst. D* **60**, 686–695.
- Winter, G. & McAuley, K. E. (2011). *Methods*, **55**, 81–93.
- Zeldin, O. B., Gerstel, M. & Garman, E. F. (2013). *J. Appl. Cryst.* **46**, 1225–1230.
- Zhang, Z., Sauter, N. K., van den Bedem, H., Snell, G. & Deacon, A. M. (2006). *J. Appl. Cryst.* **39**, 112–119.